

# ARRAY ANALYSIS OF THE GROUND VELOCITIES AND ACCELERATIONS FROM THE 1971 SAN FERNANDO, CALIFORNIA, EARTHQUAKE

BY HSUI-LIN LIU AND THOMAS HEATON

## ABSTRACT

**Profiles of ground velocity and acceleration, displayed as a function of epicentral distance, are analyzed for recordings of the 1971 San Fernando earthquake. Three long profiles (>50 km) and three short profiles (<2 km) are studied. Although there is considerable variation in waveforms and peak amplitudes observed along the long profiles, there are also many examples of coherent phases seen on adjacent stations. There are striking differences in the amplitudes and durations of ground velocity observed at stations located on hard rock sites as opposed to stations located within the large sedimentary basins of the Los Angeles area. Furthermore, the San Fernando Basin, which is adjacent to the source area, seems to respond quite differently from the Los Angeles Basin which is about 30 km from the earthquake source area. Ground acceleration profiles, however, show that there is no corresponding change in the duration or amplitude of high-frequency shaking with site characteristics. We infer that the excitation of surface waves within sedimentary basins is the reason that large peak velocities and displacements are observed for soft sites. The ground velocity waveforms are nearly identical along the three short profiles, which are all located within the Los Angeles Basin. Greater variation of waveforms and amplitudes are seen for ground acceleration along these short profiles, although strong phase coherence is still observed.**

## INTRODUCTION

The purpose of this study is to characterize the nature of ground motions recorded during the 1971 San Fernando earthquake. We systematically display the data in a fashion such that we may gain insight into wave propagation and earthquake source phenomena. Fundamental questions that we wish to address are: what is the phase coherence as a function of frequency and station spacing? What are the major phases seen in the records? And what are the effects of variations in the local seismic velocity structure (e.g., mountains and basins)? A satisfactory resolution of these questions would obviously require an extensive and very sophisticated modeling study. Instead, we have simply organized the data in a way such that simple, but hopefully meaningful, interpretations can be inferred about the nature of the ground motions produced by this earthquake.

In a study similar to this one, Hanks (1975) analyzed the ground displacements from the 1971 San Fernando strong motion data and demonstrated that there is strong coherence from station to station in the longer period waveforms. He also identified direct shear phases and subsequent surface waves at certain ranges. In this study, we extend Hanks' study (1975) by examining shorter period waveforms as represented by the ground velocities and accelerations. Ground velocity profiles are displayed together with profiles of topography and geologic structure as inferred by Yerkes *et al.* (1965). We identify possible wave types and discuss the effects of geologic structure on the amplitude and duration of the recorded ground motions.

Given the distribution of accelerometers that recorded the San Fernando earthquake, it is possible to construct ground motion profiles along three azimuths.

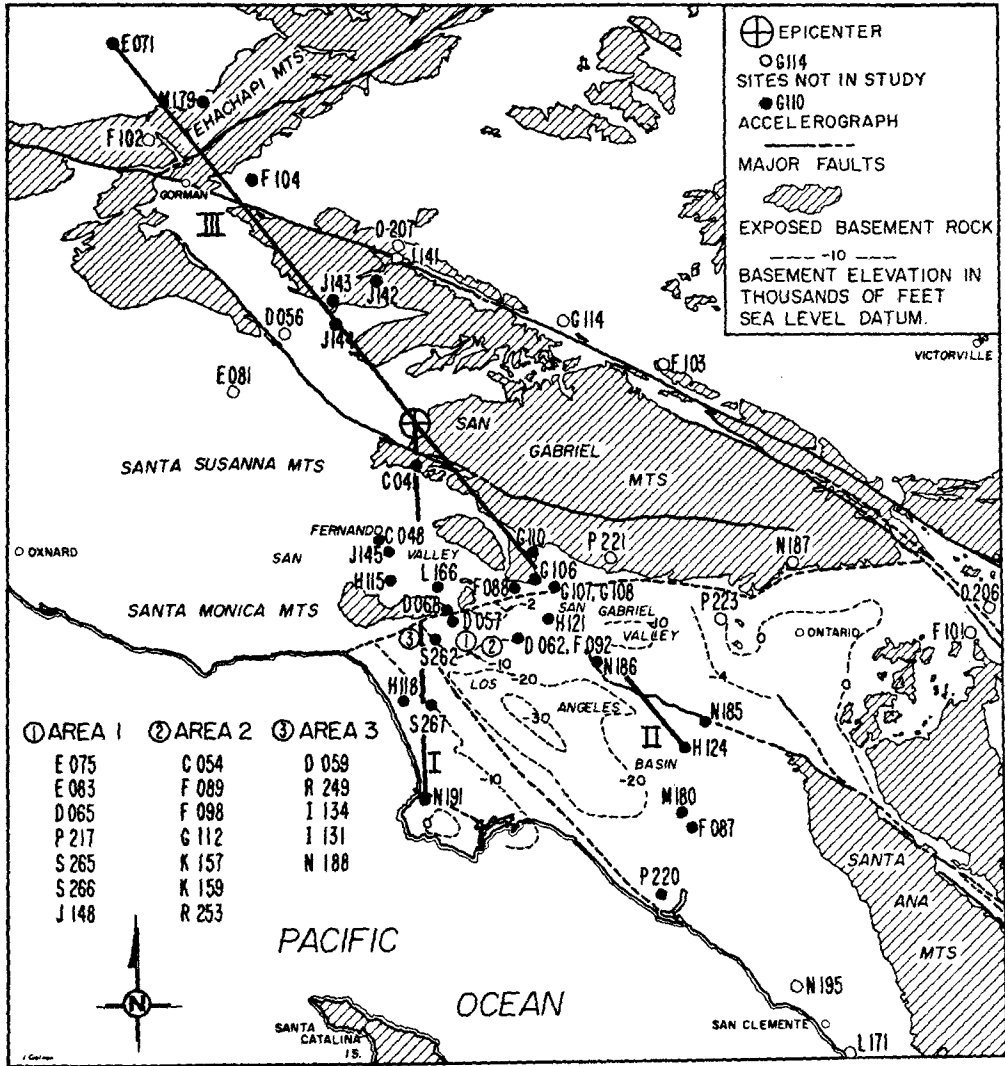


FIG. 1. The long profiles, I, II, and III, and site locations of accelerometer recordings of the 1971 San Fernando earthquake (modified from Hanks, 1975).

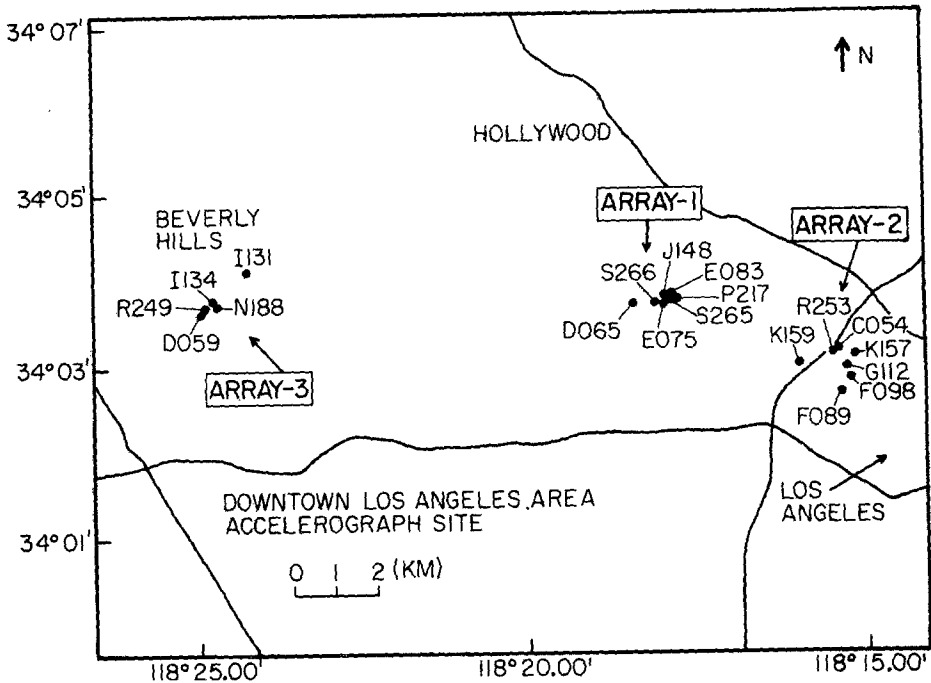


Figure 1 shows the station distribution and our corresponding profiles. All profiles originate in the epicentral region. Profile I extends 65 km southward across the San Fernando and Los Angeles basins to a station on the Palos Verdes Peninsula. Profile II extends 95 km S40°E along the front of the San Gabriel Mountains and then across the San Gabriel and Los Angeles basins. Profile III runs 90 km N40°W across the San Gabriel and Tehachapi mountains. Profile I is identical to Hanks'

TABLE 1  
S! MINUS TRIGGER TIMES

Station	Time (sec)	Station (#Fl.)	Time (sec)
Azimuth I		Local Array 1	
C041	3.0	D065 (11)	0.0
C048	1.6	E075 (11)	1.3
D057	1.1	E083 (7)	0.8
D068	0.0	J148 (17)	5.6
H115	4.0	P217 (12)	0.8
H118	0.0	S265 (31)	5.6
J145	1.6	S266 (21)	5.6
L168	1.3	Local Array-2	
N191	0.0	C054 (39)	1.3
S262	1.9	F089 (8)	5.1
S267	6.1	F098 (8)	4.5
Azimuth II		G112 (43)	1.9
G110	1.3	K157 (16)	2.7
G108	2.1	K159 (8)	4.3
G108	4.3	R253 (10)	5.6
H121	5.6	Local Array 3	
M180	0.0	D059 (19)	0.0
F087	0.0	I131 (10)	5.6
N186	0.0	I134 (15)	6.1
P220	0.0	N188 (16)	5.6
Azimuth III		R249 (27)	5.1
E071	0.0		
F102	0.0		
F104	0.0		
J142	5.0		
J143	0.0		
J144	0.0		
M179	0.0		

# Building height in terms of floors.

(1975) profile 4, and profiles II and III are somewhat abbreviated versions of Hanks' profiles 1 and 2, respectively.

The San Fernando earthquake was also well recorded by strong motion instruments in high-rise buildings. These buildings are clustered in three locations on the north side of the Los Angeles Basin: the Miracle Mile area of Wilshire Boulevard (local array 1); downtown Los Angeles (local array 2); and Century City (local array

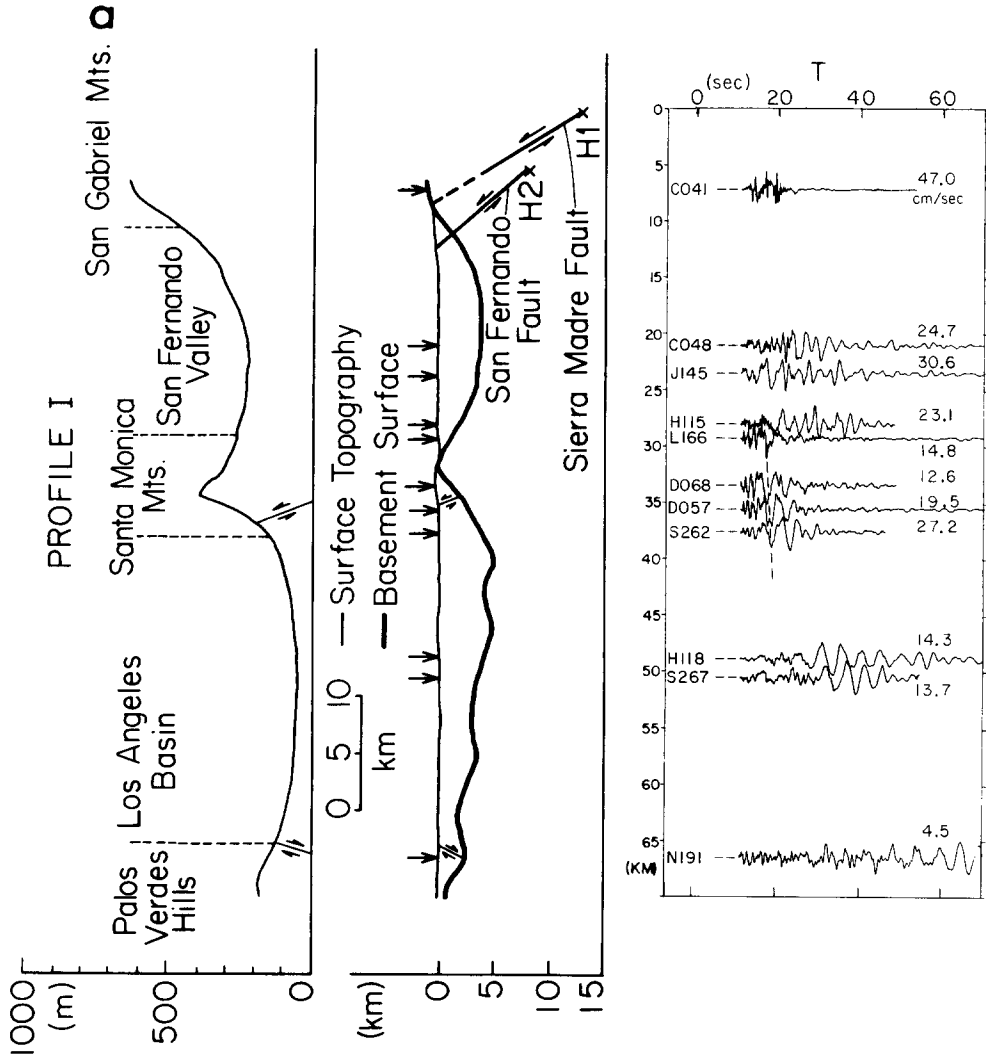


FIG. 3. Transverse, radial, and vertical components of ground velocities along profile I. The corresponding free surface and basement surface are shown to the left. Dashed lines crossing 30 and 40 km indicate the possible phase arrivals of surface waves.

3). Station locations for these dense local arrays are shown in Figure 2. These local arrays correspond exactly with Hanks' (1975) local arrays 1, 2, and 3.

Time histories of ground velocity and acceleration are all taken directly from reports published by the Earthquake Engineering Research Laboratory at Caltech (1974). Ground motions are rotated into radial, transverse, and vertical components and are then displayed as functions of time and distance from the epicenter reported by Allen *et al.* (1973). Since absolute time is not available for any records, some assumptions must be made in order to correlate phases from one station to another. We shifted records such that the apparent first shear-wave arrivals, which are named  $S_1$  by Hanks (1975), are aligned vertically in the profile.  $S_1$  minus trigger times are listed in Table 1 for all stations used in this study. Unfortunately, in some cases, the identification of  $S_1$  is very difficult, and thus some of the more distant

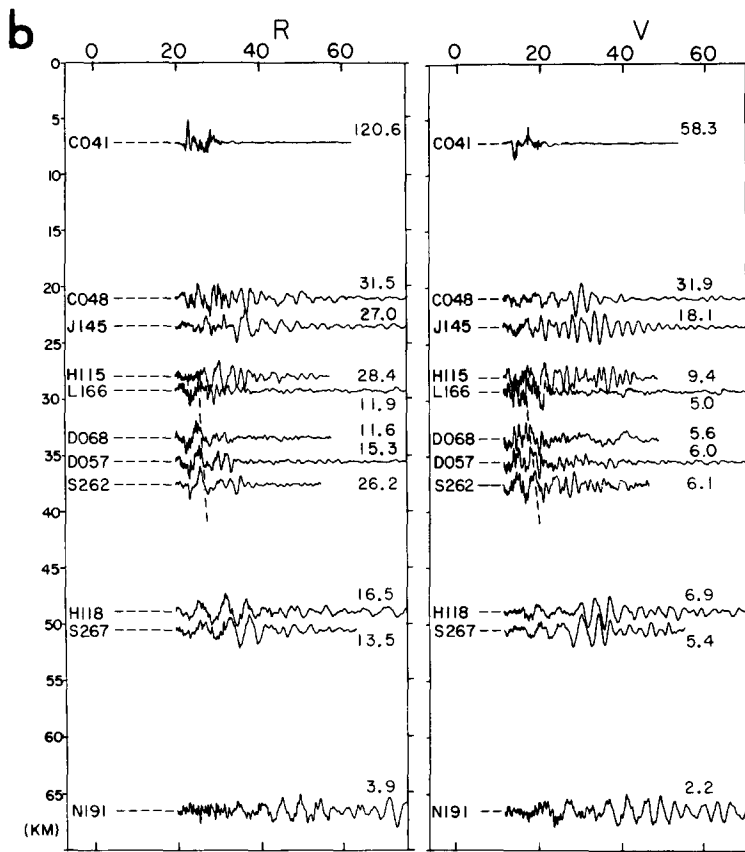


FIG. 3. Continued.

stations are probably not aligned on the first shear-wave arrival. Once the profiles are constructed, we find that the ground velocity waveforms are surprisingly coherent from station to station, allowing us to estimate apparent phase velocities, to identify possible wave types, and qualitatively separate the source from the path effects. The features of each profile will be described in more detail as follows.

### LONG PROFILES

*Profile I.* The velocity traces together with the corresponding free surface and basement surface topography profiles are displayed in Figure 3. Velocity traces begin with the  $S_1$  arrivals. From a study of both strong motion displacement waveforms and long-period teleseismic body waveforms, Heaton (1982) reported a preferred source model consisting of two approximately equal-size events.  $H1$  is the hypocenter of the first event which ruptured along the Sierra Madre fault, and 4

sec later, rupture initiated on the San Fernando fault at the second hypocenter, *H2*. According to Heaton's (1982) interpretation, the high-peak velocity observed at station C041 (Pacoima Dam) is caused by rupture directivity along the Sierra Madre fault. Although the faulting process is rather complicated, the total source duration is only about 7 sec. We believe that the signal duration at Pacoima Dam (C041) represents the approximate duration of the source.

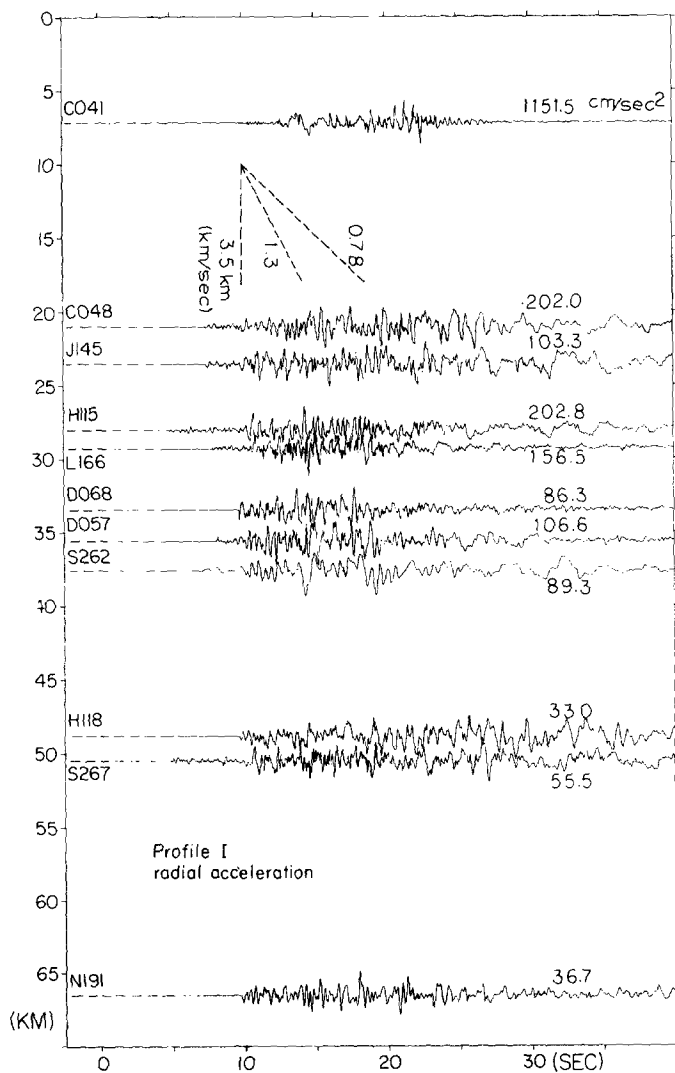


FIG. 4. Radial components of ground acceleration along profile I.

One of the most impressive features seen in Figure 3 is the correlation of ground motion waveforms with the topography of the subsurface basins. There are three stations (C048, J145, and H115) located within the San Fernando Valley. The waveforms recorded at these stations are poorly correlated and the signal durations

are about 30 sec. These durations are much longer than those seen at neighboring and more distant stations located near the Santa Monica Mountains, such as L166, D068 and D057. This contrast can be seen in Figure 3. Coherent waveforms begin to appear at station L166 and signal durations drop to about 10 sec. Furthermore, peak amplitudes drop by about one-half after passing the San Fernando Valley stations. Amplitudes increase again at stations D057 and S262 when the waves reach the Los Angeles Basin. The waveforms are quite coherent in the beginning 6 sec and there appears to be little moveout from the  $S'$  phases. The dashed lines passing stations L166, D068, D057, and S262 indicate the possible arrival of surface waves, which are characterized by gradual moveout from the  $S$  phases. They appear dispersive in nature, and Hanks (1975) demonstrates that the radial and vertical components of ground displacement are dominated by retrograde elliptical particle trajectories at these stations. At ranges of 50 km and beyond, it is hard to identify the body waves, and the waveforms appear to be well dispersed and are probably composed mainly of surface waves. The apparent moveout velocity of the surface wave phase from the  $S'$  phase is estimated to be 5.7 km/sec. If we assume that the phase velocity corresponding to the  $S'$  phase is 3.5 km/sec, then the phase velocity of these surface waves is about 2.2 km/sec.

It is useful to contrast the nature of wave propagation for waves observed in the San Fernando Valley and the Los Angeles Basin. Peak ground velocities observed in both basins are high with respect to sites in the Santa Monica Mountains. Although long-period surface waves are clearly visible in both basins, the duration of these surface waves is up to 20 sec longer in the San Fernando Valley, the basin which is closer to the earthquake source. The earthquake ruptured into the northern part of the San Fernando Valley which is a closed sedimentary basin. We hypothesize that the long signal durations are caused by surface waves which are laterally trapped within the valley. The short signal durations seen at adjacent stations in the Santa Monica Mountains indicates that these reverberating waves, which developed in the San Fernando Valley, did not propagate away from the valley.

The relatively simple waveforms observed in the Santa Monica Mountains are probably composed primarily of shear body wave arrivals. Whereas peak velocity amplitudes in the San Fernando Valley are associated with surface waves, the absence of these surface waves in the adjacent Santa Monica Mountains is probably responsible for the noticeable drop in the peak amplitude of velocity that we observe as we proceed from the San Fernando Valley into the Santa Monica Mountains. As we proceed further southward into the Los Angeles Basin, a new surface wave train appears to develop and peak velocities jump higher again with respect to those seen in the Santa Monica Mountains. It appears that the Santa Monica Mountains constitute a significant barrier across which the surface waves that developed in the San Fernando Valley and Los Angeles Basin did not propagate.

In Figure 4, we show the radial components of the ground acceleration for stations located along profile I. Traces begin at their trigger time and are aligned vertically with respect to the  $S'$  phase. Although there is considerable variation in the observed waveforms from station to station, the duration of the high-frequency motions is a fairly constant 10 sec. Furthermore, strong phases can be seen on many records at about 4 and 8 sec after the initial  $S$  arrivals. We speculate that the overall duration and timing of arrivals seen on the relatively high-frequency acceleration time history are directly related to the details of the faulting process. It is suggested that the basin geometry has less effect on these higher frequency waves.

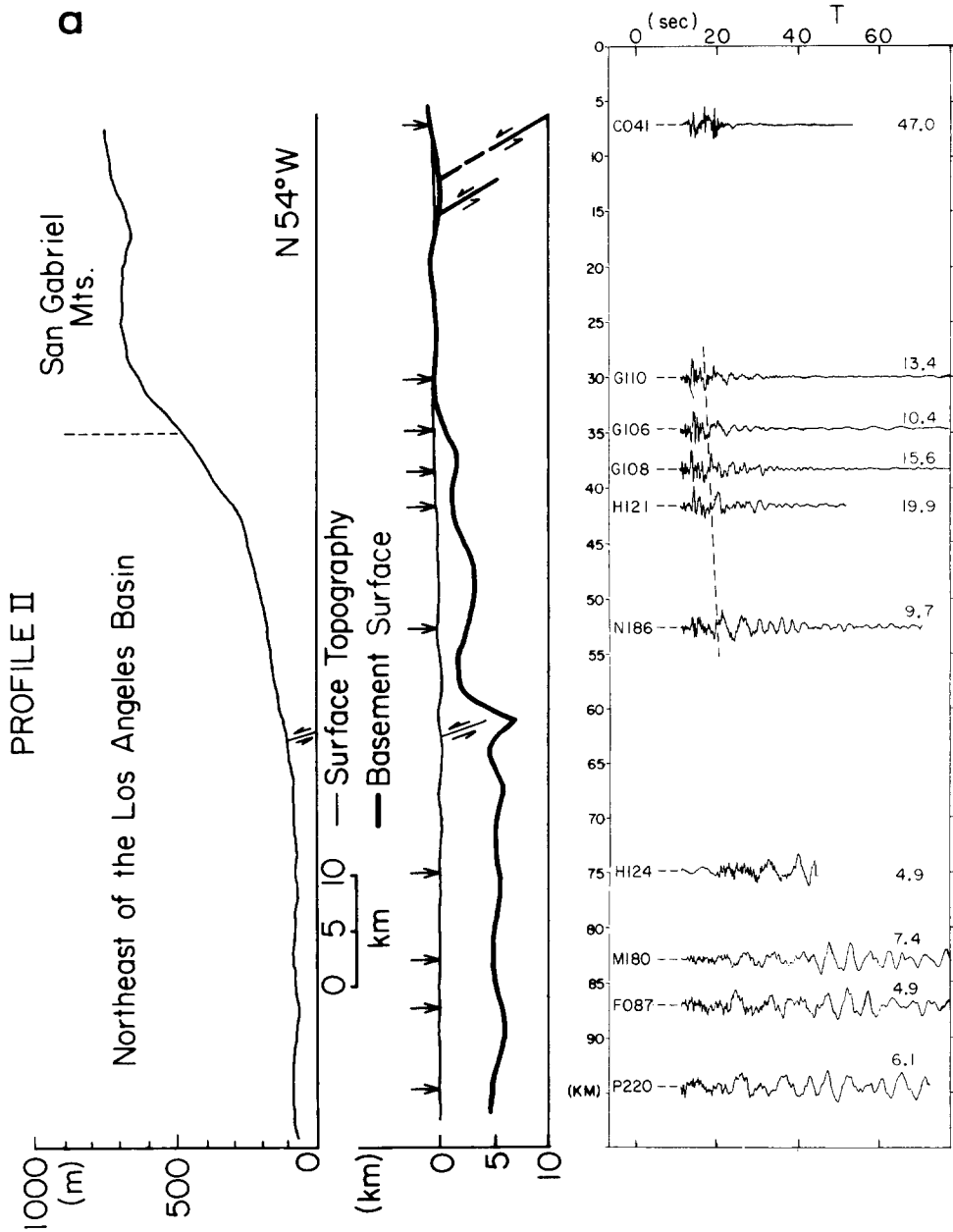


FIG. 5. Transverse, radial, and vertical components of ground velocities along profile II. The corresponding topography and the basement surface are shown to the left. Dashed lines indicate the possible phase arrivals of surface waves.

*Profile II.* Profile II runs along the southwest border of the San Gabriel Mountains and then extends across the San Gabriel basin and into the Los Angeles Basin. The velocity traces (beginning at S!) together with the path profile, are shown in Figure 5. Somewhat different features are observed along this profile. Velocity waveforms are relatively simple and have durations comparable to the source duration for stations within 40 km of the source region. Sediments are either thin or absent for these stations, and much of the waveform appears to be comprised of shear body



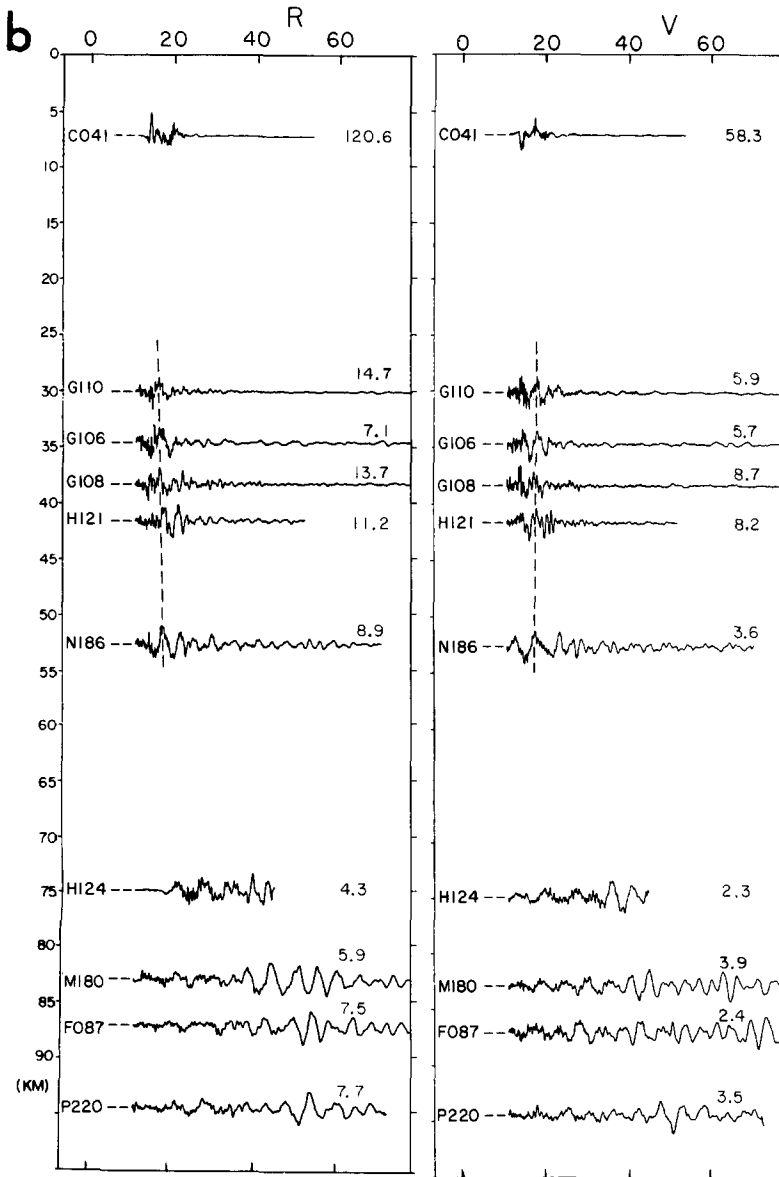


FIG. 5. Continued.

waves. However, Heaton and Helmberger (1979) show that a nondispersed fundamental Rayleigh wave may comprise a significant part of the longer period motions at these stations. The dashed lines covering the range from 30 to 50 km shows appreciable moveout of a later long-period phase with respect to the initial *S* arrivals. If we assume a horizontal phase velocity of 3.5 km/sec for the *S*<sub>1</sub> phase, then the phase velocity corresponding to the dashed line is approximately 2.7 km/sec. This is higher than the phase velocity inferred for surface waves identified in the Los Angeles Basin for profile I. This observation is consistent with the fact that sediment layers are relatively thin compared with those encountered along profile I.

Ground velocities at stations that lie in the Los Angeles Basin at distances of

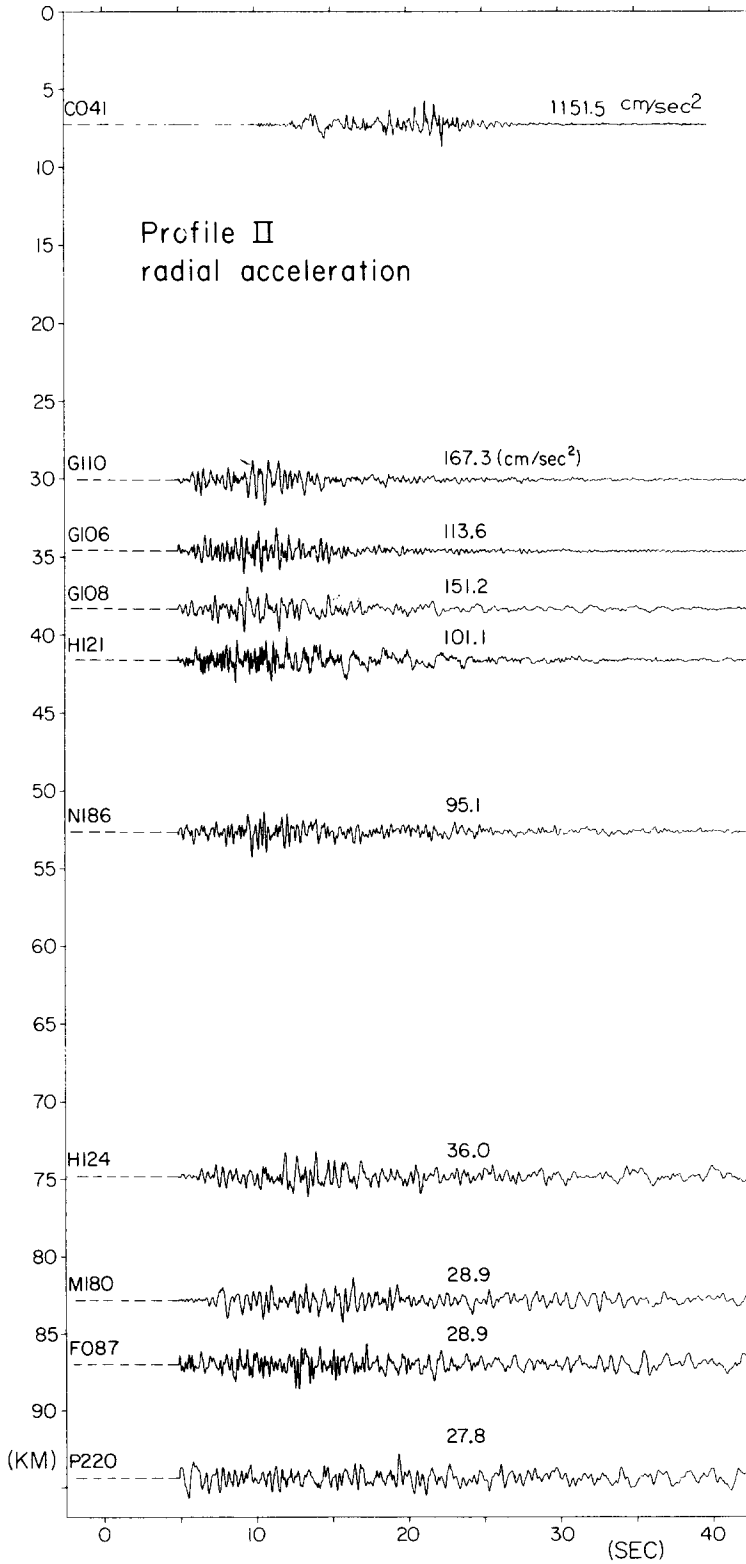


FIG. 6. Radial components of ground acceleration along profile II.

greater than 70 km consist mainly of well-dispersed surface waves. The phase *S*! cannot be clearly identified in this region. The ground motions here are similar in character to those recorded in the Los Angeles Basin in profile I.

In Figure 6, we show the radial components of the ground acceleration for stations located along profile II. Peak amplitudes and the duration of high-frequency shaking are remarkably similar to that seen along profile I. However, the strong phases seen at 4 and 8 sec in *S* wave train on profile I are not as evident in profile II. Instead, the strongest phase seen along profile II appears to be about 6 sec after the beginning of the *S* wave train.

*Profile III.* Profile III runs N40°W across mostly mountainous terrain and ground velocity traces along this profile are shown in Figure 7. Ground velocities are strikingly different along this profile from the other two profiles that cross deep sedimentary basins. The variation in the duration and amplitude of the ground velocities seems to be considerably less along this northern profile. Heaton and HelMBERGER (1979) show that displacements observed at station J142 can be reasonably modeled with a simple half-space structure. This is obviously not the case for many of the stations located along profiles I and II.

In Figure 9, we compare the peak amplitudes of radial velocity observed along the three profiles. Stations located within deep sedimentary basins are circled. It seems clear that peak velocities are larger on stations to the south, except for those stations on or adjacent to the Santa Monica or San Gabriel Mountains. It appears likely that the development of surface waves within the deep sedimentary basins is the principal reason for this amplitude variation.

In Figure 10, we compare peak radial acceleration amplitudes along the profiles. Peak accelerations are surprisingly similar for these three profiles. This is consistent with an observation previously reported by Trifunac (1976). Using data mainly from the San Fernando earthquake, he concluded that peak ground motions were greater on soft sites than on hard sites, with the effect being considerable at long periods and almost negligible at high frequencies.

#### LOCAL ARRAYS

In Figures 11, 12, and 13, we show three components of ground velocity as functions of time and epicentral distance for local arrays 1, 2, and 3, respectively. Since stations in these arrays are not generally aligned along a radial line from the epicenter, the distances shown in Figures 11 through 13 may not be indicative of the true interstation spacing.

The most obvious feature of the ground velocity is the remarkable degree of coherence across each array. Since the velocity waveforms are dominated by waves with frequencies of less than 5 Hz, we expect that most of the motion has horizontal wavelengths of greater than 0.5 km. Thus, there is good reason to expect the ground velocity to be coherent over these small arrays. However, there are several other implications of this coherence. First, the record processing must introduce very little noise into the velocity traces. This is especially impressive when one considers that the horizontal components require component rotations before they can be compared. Second, the effect of building interaction is apparently minimal on velocity waveforms. The average standard deviation of peak velocity within each array is about 12 per cent. Furthermore, it is difficult to see the systematic dependence of peak velocity on building height (see Table 1) within each array that is suggested by Boore *et al.* (1980).

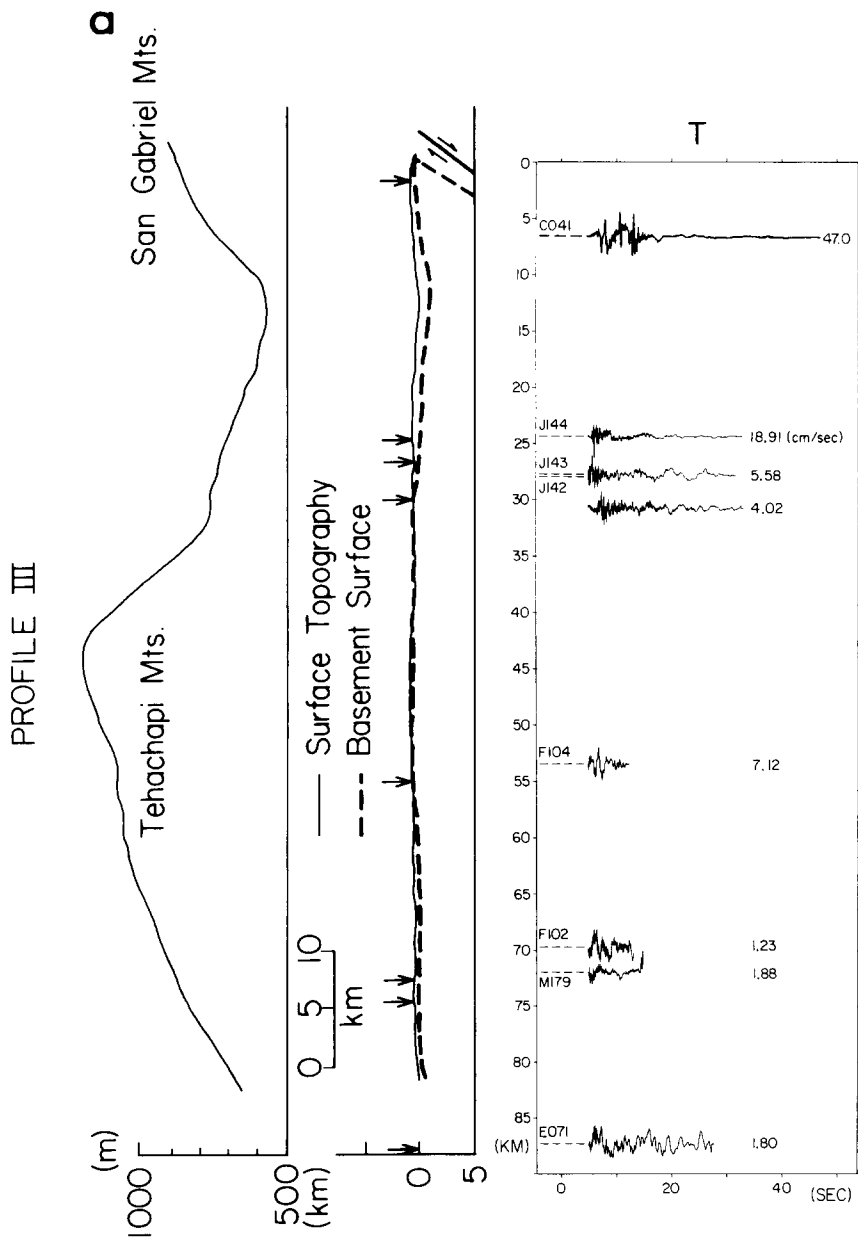


FIG. 7. Transverse, radial, and vertical components of ground velocities along profile III. The corresponding topography and the guessed basement surface are shown to the left.

We show the radial component of ground acceleration for local array 1 in Figure 14. Although less coherent than the velocities, accelerations still show strong coherence along the profile. Prominent phases can be seen at 2, 4, and 8 sec after the initial S! phase. It is difficult to see moveout of any phase for these local arrays. This is not surprising since a variation in phase velocity between 4 and 2 km/sec yields a moveout of only 0.25 sec/km. Such small time shifts could only be detected through more detailed analysis.

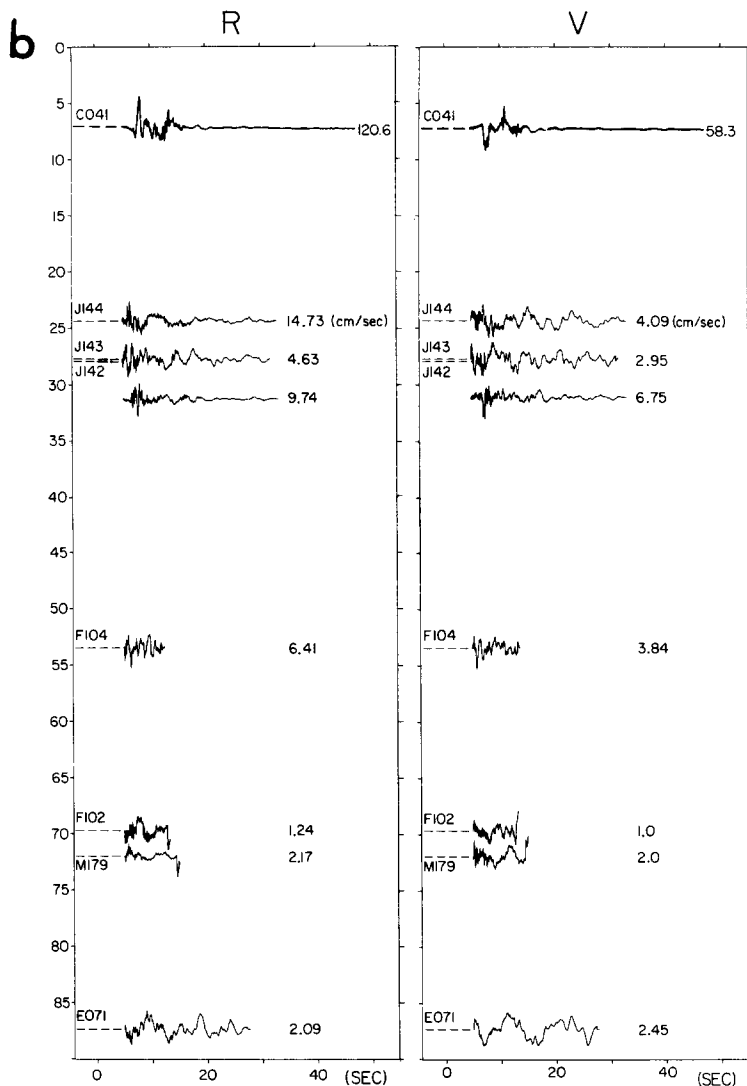


FIG. 7. Continued.

### DISCUSSION AND CONCLUSIONS

Velocity profiles recorded from the 1971 San Fernando earthquake demonstrate strong path effects due to topography of the basement surfaces. The different waveform patterns observed along three long profiles implies that valley or basin structures can produce significant reverberation and amplification effects. Higher frequency ground motions that are represented in ground acceleration profiles appear to be less affected by propagation through large sedimentary basins. The observation of Trifunac (1976) that long-period ground motions are larger at soft sites is interpreted as an effect of the development of surface waves within sedimentary basins. In the case of the San Fernando Valley, long-period surface waves

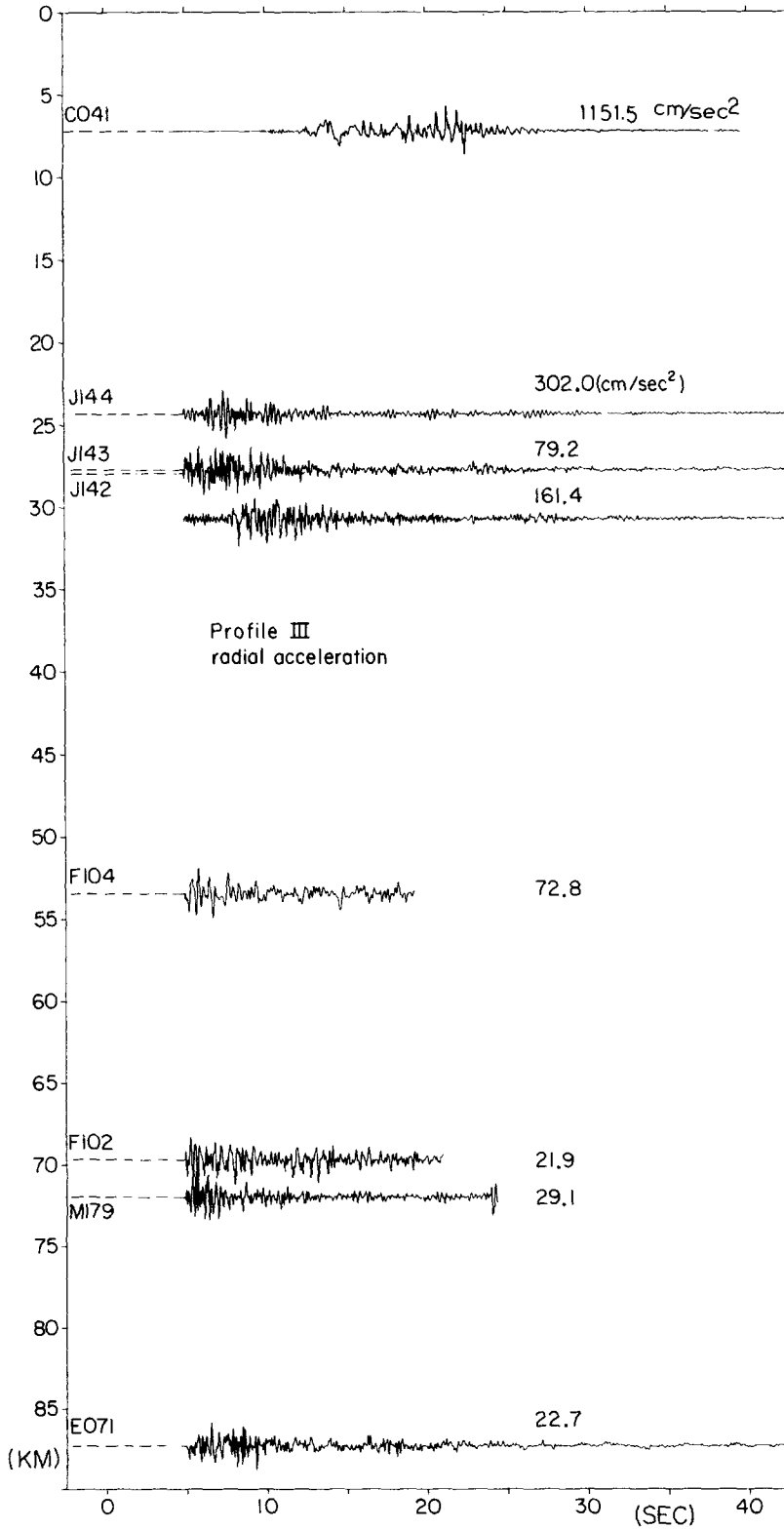


FIG. 8. Radial components of ground acceleration along profile III.

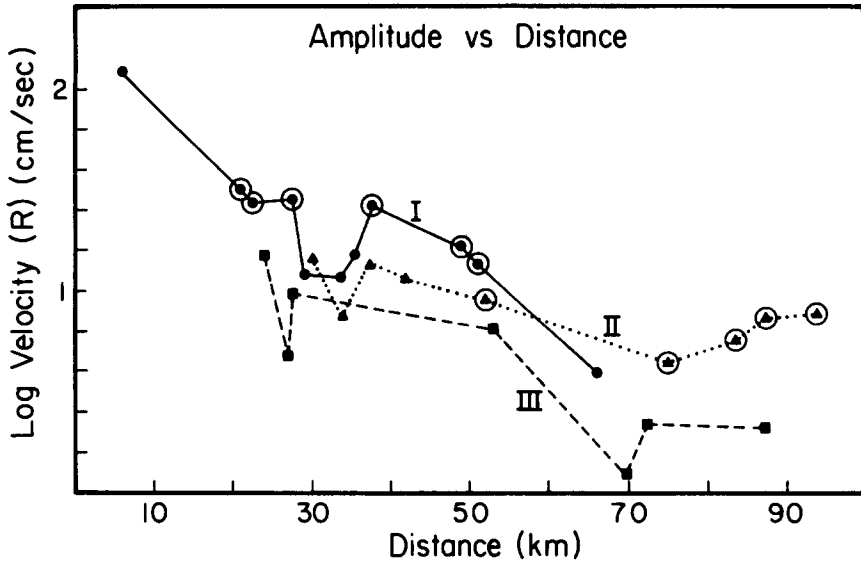


FIG. 9. Plot of the peak radial velocities as a function of epicentral distance for the three long profiles. Stations located in deep sedimentary basins are circled.

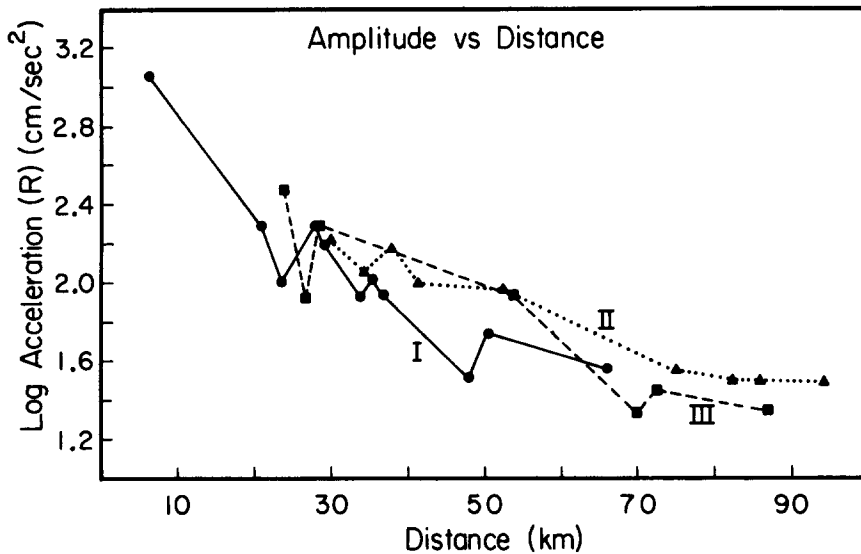


FIG. 10. Plot of the peak radial accelerations as a function of epicentral distance for the three long profiles.

appear to be trapped within this closed basin, and surface waves observed in the San Fernando Basin do not appear to propagate beyond the Santa Monica Mountains into the Los Angeles Basin.

There appear to be significant systematic variations in the ground motions from the San Fernando earthquake when they are compared with large-scale variations in geologic structure along the paths of propagation. A more complete understanding of this interaction will probably require the construction of complex three-dimensional models of both the seismic source and the propagation path. Liu (1983) has constructed simple two-dimensional, finite-difference, acoustic models that incor-

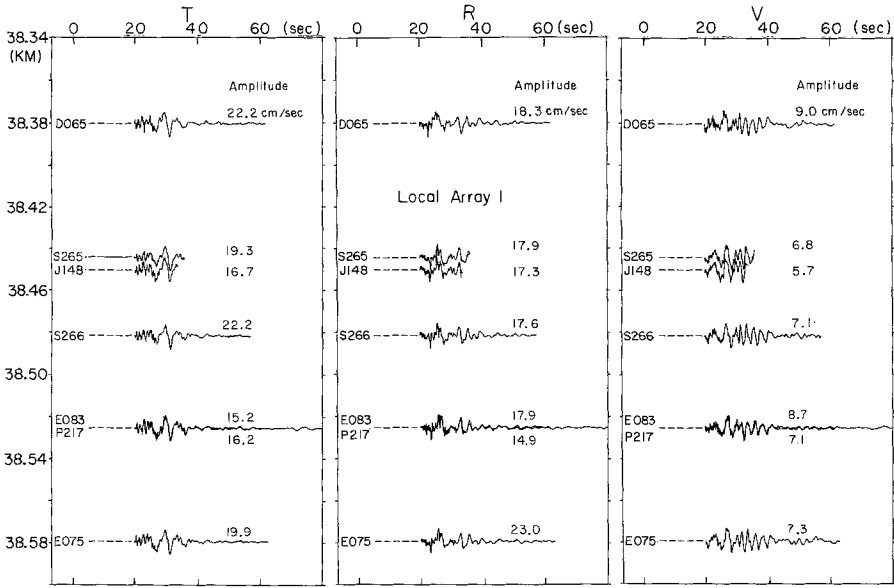


FIG. 11. Transverse, radial, and vertical components of ground velocities for local array 1.

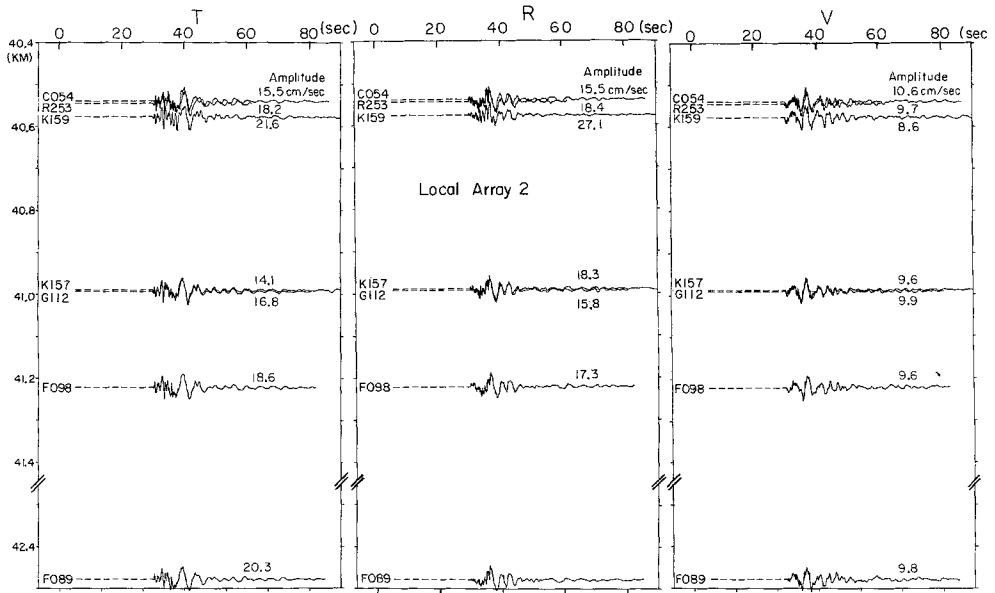


FIG. 12. Transverse, radial, and vertical components of ground velocities for local array 2.

porate several of the basic propagation path and source features assumed in this study. Modeling of this type is only appropriate for the simulation of *SH*-type arrivals, and its application to the data used in this study is limited. However, several of the features seen in the profiles presented in this study are reproduced by Liu's (1983) models. Some of the conclusions of Liu's study are: (1) the excitation of waves in the San Fernando Valley is greatest from the shallow portion of the rupture; (2) little energy from the shallow portion of the rupture is transmitted into the Santa Monica Mountains that separate the two low-velocity basins; and (3) the *S*<sub>1</sub> phase is derived mainly from the deeper part of the rupture and the presence of local basins has relatively little effect on the *S*<sub>1</sub> phase. Although many important



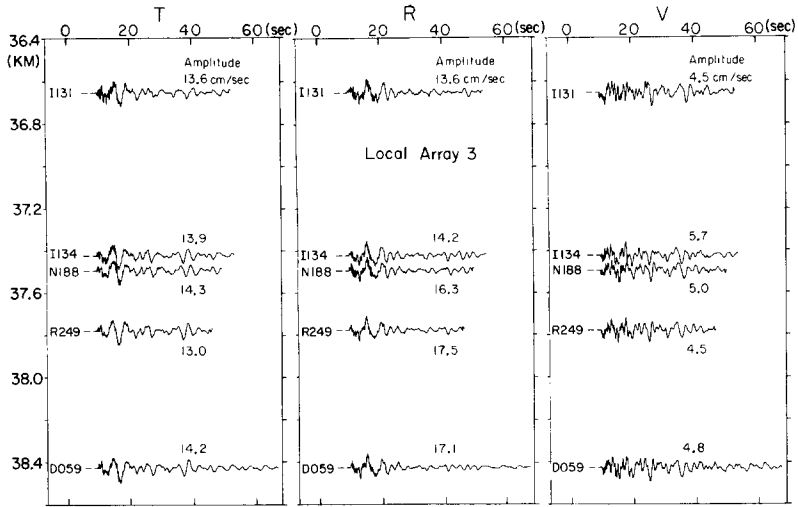


FIG. 13. Transverse, radial, and vertical components of ground velocities for local array 3.

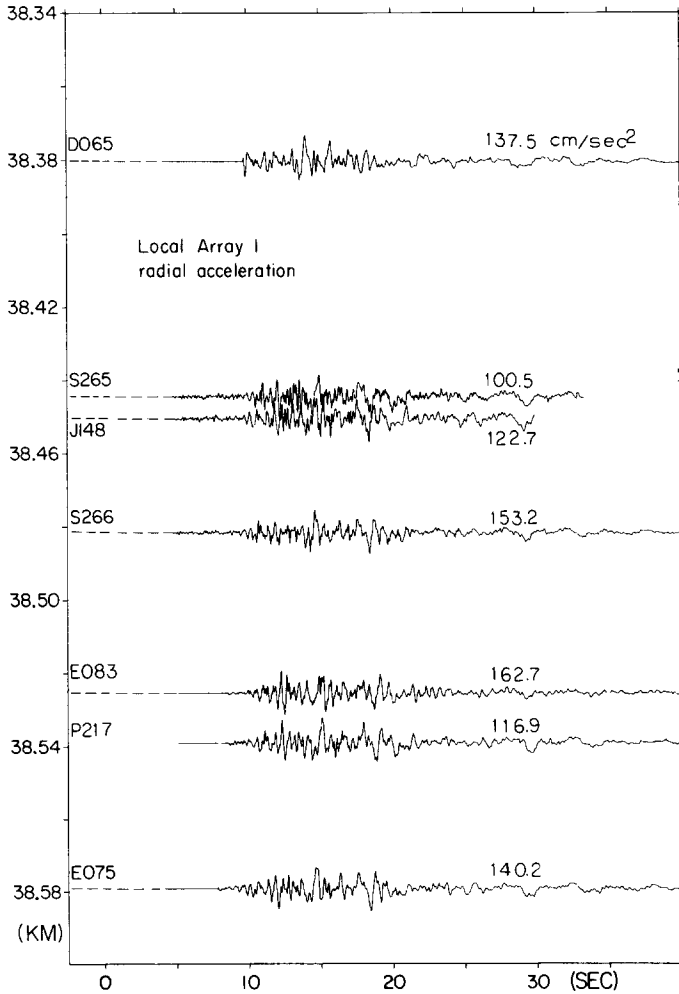


FIG. 14. Radial components of ground acceleration in local array 1.

features of the data presented in this study are still not well understood, it seems clear that the excitation of surface waves in deep sedimentary basins has a profound effect on the amplitude and duration of the ground velocities from the San Fernando earthquake. Velocity profiles along three local arrays in the Los Angeles Basin suggest that, within 3 km in range, the waveforms are almost identical. It is also suggested that higher frequency waves, as represented by ground accelerations, are less affected by these large basin structures.

#### ACKNOWLEDGMENTS

This research was supported by the National Science Foundation Grant CEE81-21719.

#### REFERENCES

- Allen, C. R., T. C. Hanks, and J. H. Whitcomb (1973). San Fernando earthquake: seismological studies and their implications in San Fernando California Earthquake of February 9, 1971, vol. I, Geological and Geophysical Studies, U.S. Government Printing Office, Washington, D.C.
- Boore, D. M., W. B. Joyner, A. A. Oliver, III, and R. A. Page (1980). Peak acceleration, velocity and displacement from strong-motion records, *Bull. Seism. Soc. Am.* **70**, 305-321.
- EERL, Caltech (1974). Strong Motion Earthquake Accelerograms, vol. II, Report from Earthquake Engineering Research Laboratory, California Institute of Technology, Pasadena, California.
- Hanks, T. C. (1975). Strong ground motion of the San Fernando California earthquake: ground displacements, *Bull. Seism. Soc. Am.* **65**, 193-225.
- Heaton, T. H. (1982). The 1971 San Fernando earthquake: a double event?, *Bull. Seism. Soc. Am.* **72**, 2037-2062.
- Heaton, T. H. and D. V. Helmberger (1979). Generalized ray models of the San Fernando earthquake, *Bull. Seism. Soc. Am.* **69**, 1311-1341.
- Liu, H. L. (1983). Interpretation of near-source ground motion and implications, *Ph.D. Thesis*, California Institute of Technology, Pasadena, California, 184 pp.
- Trifunac, M. D. (1976). Preliminary analysis of the peaks of strong ground motion; dependence of peaks on earthquake magnitude, epicentral distance, and recording site condition, *Bull. Seism. Soc. Am.* **86**, 189-219.
- Yerkes, R. F., T. H. McCulloh, J. E. Schollhamer, and J. D. Vedder (1965). Geology of the Los Angeles Basin California—an introduction, *U.S. Geol. Survey Profess. Paper 420-A*, U.S. Government Printing Office, Washington, D.C., 57 pp.

SEISMOLOGICAL LABORATORY  
CALIFORNIA INSTITUTE OF TECHNOLOGY  
PASADENA, CALIFORNIA 91125 (H.L.L.)  
CONTRIBUTION NO. 4018

U.S. GEOLOGICAL SURVEY  
SEISMOLOGICAL LABORATORY  
CALIFORNIA INSTITUTE OF TECHNOLOGY  
PASADENA, CALIFORNIA 91125 (T.H.)

Manuscript received 22 December 1983